Authors' Response to Reviews of

Aging of Droplet Size Distribution in Stratocumulus Clouds: Regimes of Droplet Size Distribution Evolution

Jung-Sub Lim and Fabian Hoffmann
Atmospheric Chemistry and Physics,

RC: ***Reviewers' Comment***, AR: Authors' Response, ☐ Manuscript Text

*All line numbers in this response letter refer to the revised manuscript unless stated.

1. Reviewer #1

RC: ***This manuscript presents a well-designed and insightful study on the evolution of droplet size distributions in maritime stratocumulus clouds, combining large-eddy simulations with a Lagrangian cloud model. The identification of two distinct DSD evolution regimes—adiabatic growth and entrainment–descent—is physically well motivated, and the emphasis on droplet history provides a compelling framework for reconciling long-standing ambiguities in the interpretation of mixing signatures.***

RC: ***The manuscript is generally well written and scientifically sound, and the proposed combined analytical–empirical formulation for relative dispersion is a valuable contribution with potential implications for cloud parameterization. However, given that much of the analysis relies critically on the Lagrangian framework and particle tracking, the paper would benefit from clearer methodological descriptions and, in some sections, deeper physical discussion to strengthen the link between simulated droplet histories and observable quantities.***

AR: We thank the reviewer for the insightful comments that have improved the quality of the paper. In response, we have clarified citations of previous studies and added a dedicated subsection detailing the particle tracking methodology, which is central to our study. Furthermore, we removed the ambiguous section noted by the reviewer. Finally, to highlight the potential implications for cloud microphysics parameterizations, we have moved the relevant material from the appendix into the main results section. We believe these revisions have made the manuscript more precise and insightful. Please refer to our point-by-point author's response below.

RC: ***The authors need to provide more detailed descriptions of the specific implementation of particle trajectory tracking, as a substantial portion of the analyses in this manuscript is based on this method.***

AR: As the particle tracking implementation is an important component of our analysis, we have revised the manuscript to include a detailed section dedicated to these methods. Please refer to Section 2.3 in the revised manuscript:

> To explicitly resolve the microphysical histories of individual droplets, we implemented a Lagrangian particle-tracking algorithm within the L^3 model. Each LCM particle is assigned a unique identifier (ID) upon initialization, which is preserved throughout its lifecycle. For this study, we tracked 400 particles. At initialization, four distinct and equidistantly spaced vertical columns were selected across the domain. Within each column, one particle was randomly chosen from each of the lowest 100 vertical grid boxes, yielding 100 tracked particles per column. To manage data volume and focus

exclusively on in-cloud evolution, we applied a conditional recording scheme: data were recorded only when a flagged particle resided within a grid box classified as cloudy ($q_c \geq 0.01$ g kg^{-1}). We used the first 3 h as a spin-up period, during which the flagged particles were dispersed by boundary-layer turbulence and became nearly well mixed within the boundary layer. Particle output was then enabled, and the final 2 h are used for analysis (Sec. 2.2).

These tracked particles function as 'virtual observers', although they remain microphysically active, undergoing condensation and evaporation indistinguishable from the standard LCM particles. At each time step, ~~the properties of the LES grid box (e.g., pressure, temperature, vapor pressure) and those of the LCM particles (e.g., droplet radius~~ they sample the local thermodynamic conditions and record the bulk microphysical statistics of the droplet ensemble within their resident grid cell. Since particles typically undergo multiple cycles of entrainment and detrainment driven by turbulent vertical circulations, they often re-enter the cloud layer several times. Consequently, the effective number of in-cloud records is larger than the number of tracked LCM particles.

The recorded dataset includes each particle's Lagrangian state vector (unique ID, radius r, multiplicity, supersaturation fluctuation S', three-dimensional velocity components, and position) ~~within~~ together with the co-located Eulerian state variables, including pressure p, turbulent kinetic energy dissipation rate ε, LES gridbox mean supersaturation S, temperature T, and water vapor mixing ratio q_v. Additionally, properties derived from the full droplet population within the grid box, including q_c, cloud droplet number concentration N_c, supersaturation standard deviation σ_S, r_m, and d_r, were calculated and stored alongside the particle data. This approach ensures that the ~~same grid boxare recorded. Note that properties along the LCM particle trajectories are~~ dataset captures the complete microphysical context of droplets, specifically during their residence in the cloud, filtering out the dry aerosol phase.

The resulting trajectories are recorded at a sampling interval equivalent to the model timestep ($\delta t = 0.5$ s). To mitigate the high-frequency noise inherent to Lagrangian trajectories in turbulent flows, these properties were smoothed using a Gaussian kernel filter (Virtanen et al., 2020) ~~,~~with a window size of 10 s ~~to reduce noise~~during post-processing.

RC: ***The authors use the mean radius (r_m) for their analysis, whereas many previous studies (including those cited by the authors) have used the volume-mean radius (r_v). Although the results may be similar, the authors should explicitly clarify the differences between these two definitions to avoid inaccurate citation of the literature and potential misunderstanding by readers.***

AR: We appreciate the reviewer pointing this out. We agree that clarifying the difference between mean radius (r_m) and volume-mean radius (r_v) is crucial to avoid misunderstanding. We have revised the manuscript to explicitly distinguish between these definitions. Furthermore, we have corrected our citations to reflect the specific metrics used in previous works: r_v was used by Chandrakar et al. (2018) and Lu et al. (2020), while r_m was used by Luo et al. (2022).

Previous studies ~~have shown~~ indicate that the correlation between d_r and ~~r_m varies depending on the~~ mean droplet size varies with dominant microphysical processes and environmental conditions~~. In particular, this correlation can shift~~ , often shifting between positive and negative across different stages of droplet evolution (Chandrakar et al., 2018; Lu et al., 2020; Luo et al., 2022). ~~For instance, in~~ We note that some prior studies utilize the volume-mean radius ($r_v = \langle r^3 \rangle^{1/3}$), which is weighted toward larger droplets (Chandrakar et al., 2018; Lu et al., 2020). While $r_v \geq r_m$, both metrics generally capture

similar evolutionary trends in this context.

1.1. Line 115: Mixing fraction definition and alternative using θ_l

RC: ***The mixing fraction used here is not newly defined; Equation (3) is a variant of the moisture conservation equation (see Yang et al. (2016) and Lu et al. (2018)). In addition, I am curious about how the mixing fraction would behave if it were calculated using the conservation equation of liquid water potential temperature.***

AR: We apologize for any confusion caused by the phrasing. We did not intend to claim Equation (3) as a novel definition, but rather to specify that we adopted this specific formulation among various methods for calculating the mixing fraction. Therefore, we have revised the text to clearly state that this definition follows established methods, and we have added citations to Yang et al. (2016) and Lu et al. (2018) as suggested.

> Based on the sharp contrast in q_{t} and θ_{l} between the boundary layer and the free troposphere, we ~~define~~ adopt a mixing fraction,
>
> $$\chi = \frac{(q_{\mathrm{t}} - q_{\mathrm{t,bl}})}{(q_{\mathrm{t,ft}} - q_{\mathrm{t,bl}})}, \tag{1}$$
>
> which represents the fraction of free-tropospheric air mixed with boundary-layer air ~~. In this simulation,~~ (Yang et al., 2016; Lu et al., 2018). While calculating χ ~~is estimated using~~ using θ_{l} yields results highly correlated with those based on q_{t}, ~~where~~ we select q_{t} as the conserved variable because it exhibits a more constant profile in the free troposphere (Fig. 3a), making the choice of representative free-troposphere value easier.

AR: Regarding the reviewer's question about using liquid water potential temperature (θ_l), we performed a sensitivity analysis and confirmed that calculating the mixing fraction using θ_l yields results that are highly correlated with the q_t-based definition (r$>$ 0.78; Fig. AR1c and d). However, we explicitly chose q_t as the conserved variable because it offers a more robust definition. As shown in Fig. 1a, q_t exhibits a more constant vertical profile in the free troposphere compared to θ_l, which can be subject to radiative cooling effects near the cloud top. Therefore, using q_t minimizes ambiguity in defining the reference states and effectively represents the mixing state of the system without loss of generality.

1.2. Section 3.4: Optical properties and Figure 13

RC: ***While the authors attempt to analyze the potential effects of DSD aging on optical properties, the presentation of Figure 13 may lead to confusion. Despite the pronounced regional differences in DSD evolution shown earlier, these differences are not evident in Figure 13. The authors may wish to reconsider the necessity of this section. If Figure 13 is kept, additional discussion on the impacts of regional DSD evolution on optical properties is required.***

AR: We agree with the reviewer that Figure 13 did not effectively convey the regional differences in DSD evolution and could lead to confusion regarding the link to optical properties. To avoid ambiguity and maintain a sharper focus on the core Lagrangian analysis of DSD aging regimes, we have decided to remove this section and the corresponding figure from the revised manuscript.

AR: Instead, we have moved the content from the Appendix to the last section of the results. This section presents the combined equation for the trajectory derived from the analytical solution suggested by Liu, Daum, and Yum (2006) and the empirical fit we observed. As noted by the reviewer, this "proposed combined

analytical–empirical formulation for relative dispersion is a valuable contribution with potential implications for cloud parameterization."

References

Chandrakar, K. K., Cantrell, W., & Shaw, R. A. (2018). Influence of turbulent fluctuations on cloud droplet size dispersion and aerosol indirect effects. *Journal of the atmospheric sciences*, *75*(9), 3191–3209.

Liu, Y., Daum, P. H., & Yum, S. S. (2006). Analytical expression for the relative dispersion of the cloud droplet size distribution. *Geophysical research letters*, *33*(2).

Lu, C., Liu, Y., Yum, S. S., Chen, J., Zhu, L., Gao, S., ... Wang, Y. (2020). Reconciling contrasting relationships between relative dispersion and volume-mean radius of cloud droplet size distributions. *Journal of Geophysical Research: Atmospheres*, *125*(9), e2019JD031868.

Lu, C., Sun, C., Liu, Y., Zhang, G. J., Lin, Y., Gao, W., ... Jin, L. (2018). Observational relationship between entrainment rate and environmental relative humidity and implications for convection parameterization. *Geophysical Research Letters*, *45*(24), 13–495.

Luo, S., Lu, C., Liu, Y., Li, Y., Gao, W., Qiu, Y., ... others (2022). Relationships between cloud droplet spectral relative dispersion and entrainment rate and their impacting factors. *Advances in Atmospheric Sciences*, 1–20. doi:

Virtanen, P., Gommers, R., Oliphant, T. E., Haberland, M., Reddy, T., Cournapeau, D., ... SciPy 1.0 Contributors (2020). SciPy 1.0: Fundamental Algorithms for Scientific Computing in Python. *Nature Methods*, *17*, 261–272. doi:

Yang, F., Shaw, R., & Xue, H. (2016). Conditions for super-adiabatic droplet growth after entrainment mixing. *Atmospheric Chemistry and Physics*, *16*(14), 9421–9433.

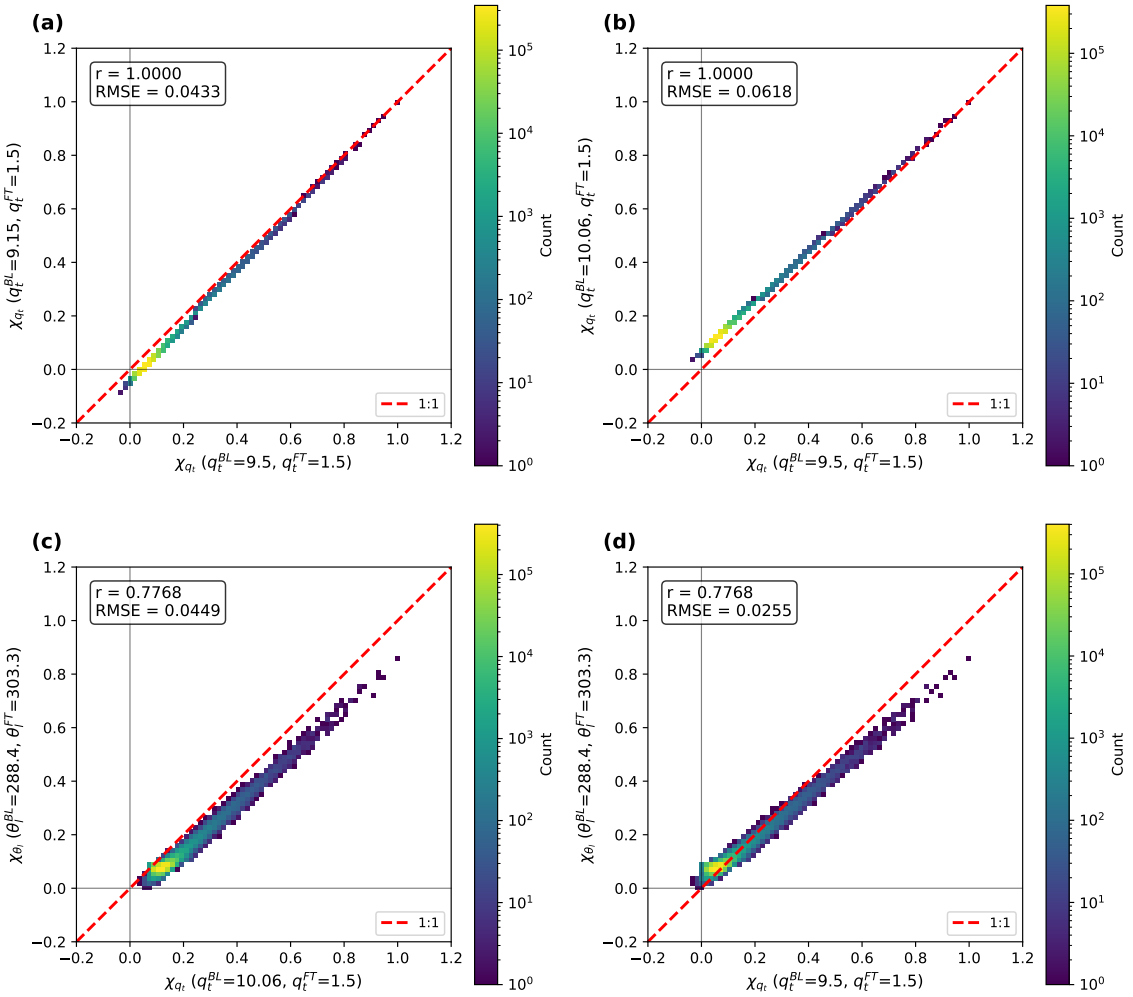

Figure AR1 Comparison of mixing fractions (χ) derived from different thermodynamic variables and reference boundary layer value (q_t^{BL}). (a, b) Sensitivity of the mixing fraction calculated from total water mixing ratio (χ_{q_t}) to variations in different boundary layer (q_t^{BL}) values with fixed free troposphere (q_t^{FT}) value. (c, d) Scatter density plots comparing mixing fractions derived from liquid water potential temperature (χ_{θ_l}) versus those derived from total water mixing ratio (χ_{q_t}). The color shading represents the sample count on a logarithmic scale. The red dashed line indicates the 1:1 relationship. The Pearson correlation coefficient (r) and root-mean-square error (RMSE) are provided for each comparison.